

1-1-1979

The reoxidation of reduced silicon dioxide films fixed charges and growth kinetics.

Cheonq-Fat Chan

Follow this and additional works at: <http://preserve.lehigh.edu/etd>

 Part of the [Electrical and Computer Engineering Commons](#)

Recommended Citation

Chan, Cheonq-Fat, "The reoxidation of reduced silicon dioxide films fixed charges and growth kinetics." (1979). *Theses and Dissertations*. Paper 1873.

This Thesis is brought to you for free and open access by Lehigh Preserve. It has been accepted for inclusion in Theses and Dissertations by an authorized administrator of Lehigh Preserve. For more information, please contact preserve@lehigh.edu.

THE REOXIDATION OF REDUCED SILICON DIOXIDE FILMS-
FIXED CHARGES AND GROWTH KINETICS

by

Cheong-Fat Chan

A Thesis

Presented to the Graduate Committee

of Lehigh University

in Candidacy for the Degree of

Master of Science

in

Electrical Engineering

Lehigh University

1979

ProQuest Number: EP76145

All rights reserved

INFORMATION TO ALL USERS

The quality of this reproduction is dependent upon the quality of the copy submitted.

In the unlikely event that the author did not send a complete manuscript and there are missing pages, these will be noted. Also, if material had to be removed, a note will indicate the deletion.



ProQuest EP76145

Published by ProQuest LLC (2015). Copyright of the Dissertation is held by the Author.

All rights reserved.

This work is protected against unauthorized copying under Title 17, United States Code
Microform Edition © ProQuest LLC.

ProQuest LLC.
789 East Eisenhower Parkway
P.O. Box 1346
Ann Arbor, MI 48106 - 1346

CERTIFICATE OF APPROVAL

This thesis is accepted and approved in partial fulfillment of the requirements for the degree of Master of Science in Electrical Engineering.

Sept. 20, 1979
(date)

Professor in Charge

Chairman of Department

Acknowledgements

The author writes to express his deepest gratitude and respect to his advisor, Professor Frank H. Hielscher, for introducing the author to the many facets of Solid State Technology. His suggestions and discussions throughout the study is also deeply appreciated.

TABLE OF CONTENTS

	Page
Abstract.	1
1. Introduction.	3
2. MOS Capacitor.	5
3. Experimental Details	
3.1 Fabrication of MOS Capacitors.	14
3.2 Oxidation.	14
3.3 Reduction.	15
3.4 Reoxidation.	15
3.5 Gate Electrode Metallization	17
3.6 Deposition of Back Metal Contact	17
3.7 Measurement of Fixed Charge.	17
4. Results	19
4.1 Peak Oxide Charge.	19
4.2 Non-Growth Time.	21
4.3 Final Oxide Charge	24
4.4 Fast Surface States.	27
5. Discussion.	30
5.1 Model for Peak Oxide Charge.	30
5.2 Model for Non-Growth Time.	34
5.3 Final Charge	37
Appendix A-Cleaning of Si Wafers.	38
Appendix B-Oxygen Partial Pressure Chart	39
Appendix C-Oxygen Diffusion in SiO ₂	41
References	42
Vita.	43

LIST OF FIGURES

		Page
Fig. 1A	An MOS Capacitor	6
Fig. 1B	Energy Band Diagram of Ideal MOS Structure .	6
Fig. 2	Energy Band Diagrams of an MOS Capacitor for all Indicated Conditions.	7
Fig. 2A	Accumulation	7
Fig. 2B	Depletion	7
Fig. 2C	Inversion.	7
Fig. 3	Effect of Fixed Positive Charge on Ideal CV Curve	9
Fig. 4A	Effect of Charge Within the Insulator (no external bias).	11
Fig. 4B	Effect of Charge Within the Insulator (flat band condition)	11
Fig. 4C	Effect of an Arbitrary Space Charge Distribution Within the Insulator	12
Fig. 5	Gas Mixture for the Reduction System	16
Fig. 6	Experimental Setup for CV Measurement . . .	18
Fig. 7	Charge Density as a Function of Reoxidation Time.	20
Fig. 8	Peak Time as a Function of Oxygen Partial Pressure.	22
Fig. 9	Nongrowth Time as a Function of Oxygen Partial Pressure.	23
Fig. 10	Final Charge Density as a Function of Oxygen Partial Pressure	25
Fig. 11	Oxide Thickness as a Function of Time. . . .	26
Fig. 12	Distortion of CV Curves	28
Fig. 13	Charge Density as a Function of Oxygen Partial Pressure.	29
Fig. 14A	Charge Density as a Function of Time	31
Fig. 14B	SiO ₂ -Si Charge Distribution Before Reoxidation	31
Fig. 14C	SiO ₂ -Si Charge Distribution After Reoxidation	31

LIST OF FIGURES

	Page
Fig. 15 Oxygen Partial Pressure as a Function of Flow Rate.....	40

LIST OF TABLES

	Page
Table I- Peak Time and ΔQ_p	32
Table II-Oxygen Diffusion in SiO_2	33
Table III-Nongrowth Time and ΔQ_2	35
Table IV-Effective Diffusion Coefficient	36
Table V- Oxygen Partial Pressure	39

Abstract

Silicon dioxide films thermally grown on silicon contain positive charge near the silicon dioxide/silicon interface. This charge can be increased by exposure of the oxide films to low oxygen partial pressure atmospheres, for example in ambients containing mixtures of CO and CO₂.

Capacitance-voltage measurements at room temperature on the reduced oxides (oxides exposed to low oxygen partial pressure atmospheres) have demonstrated that the oxide fixed charge increases gradually with decreasing oxygen partial pressure (increasing CO/CO₂ ratio). This increase of charge is believed to be caused by the creation of oxygen vacancies.

The observed increases in these quantities may be eliminated by reoxidizing the reduced samples at an elevated temperature in dry oxygen.

In this study, the oxide charges following reoxidation have been examined in detail on oxides which were initially reduced at different partial pressures. It was found that during the beginning of the reoxidation process the charge increased followed by a gradual decrease to values approaching those found in unreduced oxides. Reduced oxides have shown a non-growth time during the reoxidation, this time ranging from a minute to 200 minutes for samples reduced at different partial pressures. After this time

1a) the reduced oxides were found to grow again, at the same rate as an unreduced oxide.

The time required for the charges to reach their peak, the non-growth time, and the final interface charges were all found to be a function of the reducing partial pressure. A qualitative model is proposed to explain these observations.

1. Introduction

MOS structures play a very important role in today's technology. The majority of Random Access Memory (RAM) and Read Only Memory (ROM) use MOS structures because of their low power consumption and high density (more bits per cm^2). Electrically Programmable Read Only Memory (EPROM) can only be built with MOS structures.

Silicon dioxide is the most widely used insulator for MOS devices. It is well known that there exists a built-in positive charge in the oxide regardless of growth conditions.^[1-4] Even at the present level of technology, the Si-SiO₂ interface is not very well understood. For instance, a positive charge always resides in the oxide near the silicon interface; despite numerous studies, the origin of this fixed charge remains somewhat obscure. One proposed explanation for this charge is that it originates at positively charged impurity centers, such as Na. However, it was shown by Revesz^[5] and Evans that Na is not likely to be the major cause of this charge in most oxide films. Deal,^[2] Fowkes and Hess^[3,6] have suggested that this fixed charge may be due to an increased ratio of silicon to oxygen at the Si-SiO₂ interface, and that charged oxygen vacancies are formed near the interface during oxidation.

Fowkes and Hess^[3] have purposely altered the stoichiometry of the silicon dioxide layer by exposing it to a reducing ambient

of CO-CO₂ at an elevated temperature (910° C), which was found to increase the positive oxide charge and the surface state density through the assumed creation of charged oxygen vacancies. Fowkes and Kiddon^[7] have also studied the effects of different partial pressures and temperatures on oxide charge, whereas Pike^[8] has concentrated on the reoxidation kinetics of oxides previously reduced in a CO-CO₂ ambient.

Pike investigated the reoxidation process of oxides reduced at 7×10^{-17} oxygen partial pressure. His results can be summarized as follows:

- 1) Upon reoxidation, the charge of a reduced sample is shown to peak initially and then to gradually decrease with time.
- 2) The reduced oxides had a non-growth time of about 200 minutes.
- 3) After the non-growth time, the oxides grew at a normal rate and the charge was reduced to that of previously unreduced samples.

The goal of the present investigation is to gain additional insight into the origin and properties of the oxide charge through a detailed examination of the reoxidation kinetics of oxides reduced in different partial pressures. Since the reduction process is believed to result in oxygen vacancies, the effects of filling these charge centers during reoxidation was monitored by measurement of the flat band voltage of MOS capacitors and the oxide

film thickness versus reoxidation time.

2. MOS Capacitor

One of the most useful structures customarily employed in the study of surface effects and of the characteristics of surface space charge regions is the metal oxide semiconductor capacitor shown in Fig. 1A.

An important difference exists between the MOS capacitor structure and most other semiconductor structures, in that there exists no dc current flow across the space charge layer. Thus, the surface space charge region will be in thermal equilibrium and the Fermi level will be constant throughout the surface space charge layer. The energy band diagram of an ideal MOS capacitor on an n-type silicon substrate is shown in Fig. 1B. For convenience, the silicon substrate will be considered as the reference electrode. One of the distinct characteristics of MOS capacitors is that the space charge region in the silicon may be altered by varying the applied bias on the gate electrode. If a voltage is applied to the gate, the following cases may be distinguished for the MOS capacitor (Figs. 2A, 2B, 2C). Regardless the value of the gate voltage, the Fermi level in the semiconductor remains constant, since equilibrium holds.

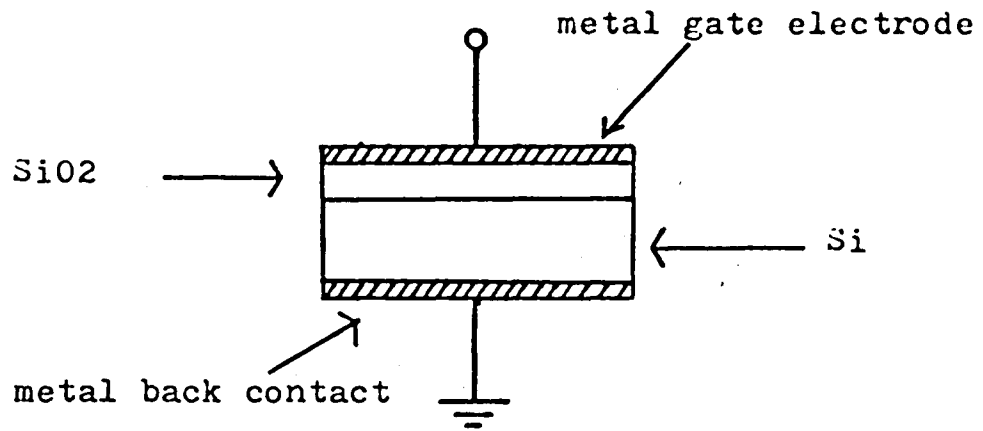


Fig. 1 A MOS capacitor .

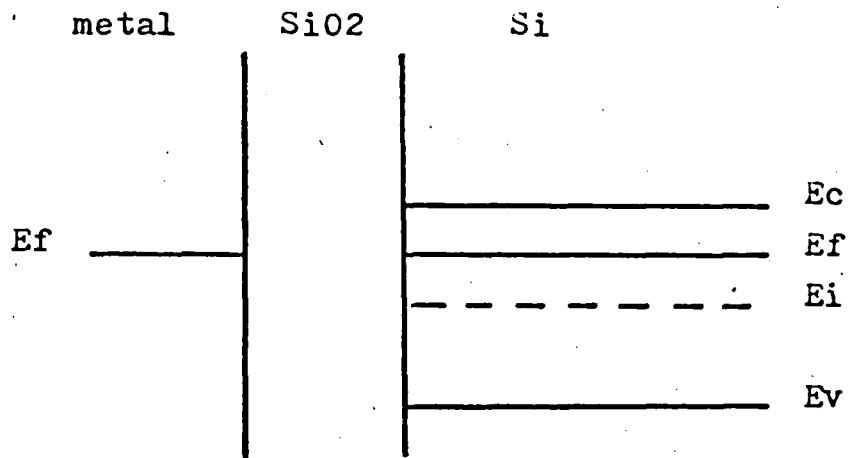


Fig. 1b Energy band diagram of the ideal MOS structure .

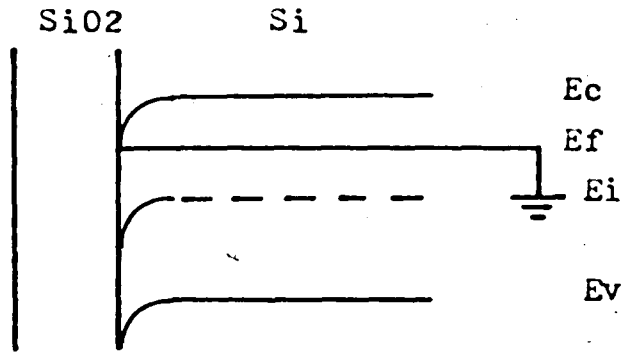


Fig. 2A Accumulation .

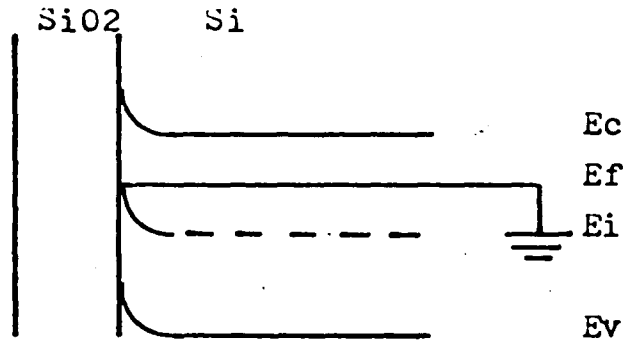


Fig. 2B Depletion ..

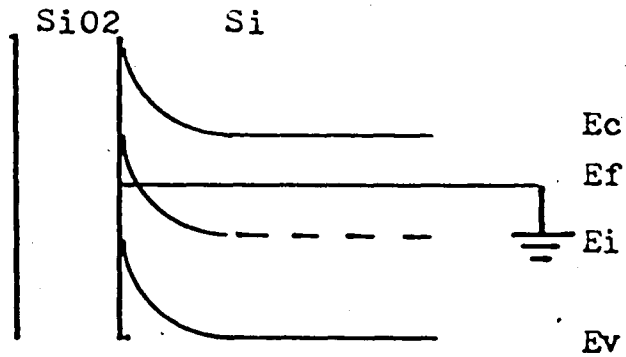


Fig. 2C Inversion .

Fig. 2 Energy band diagrams of an MOS capacitor for all indicated conditions.

- 1) Positive voltage: the positive potential will attract a negative charge in the semiconductor which accumulates near the oxide-silicon interface (accumulation).
- 2) Small negative voltage: a positive charge will be induced in the semiconductor, which is due to electrons being pushed away from the vicinity of the interface, leaving behind a depletion region consisting of uncompensated donors. This is known as the depletion condition .
- 3) Large negative voltage: if the applied voltage is increased, the energy bands bend downward and all majority carriers are depleted. Eventually when the conduction band comes close to the Fermi level, the concentration of electrons near the surface will increase very sharply. The device is then in strong inversion.

It is well known that SiO_2 is not a perfect insulator. SiO_2 contains mobile impurity ions, fixed charges and chargeable interface states, all of which will affect the electrical characteristics of the Si- SiO_2 interface.

Experiments with MOS capacitors showed the existence of a fixed charge, apparently located in the SiO_2 near the SiO_2/Si interface. This charge results in a parallel shift of flat band voltage as shown in Fig. 3. Consider a sheet charge per unit area within the SiO_2 as shown in Fig. 4A. Under the condition of zero bias this sheet charge will induce an image charge partly in the metal and partly in the semiconductor. If we neglect the work

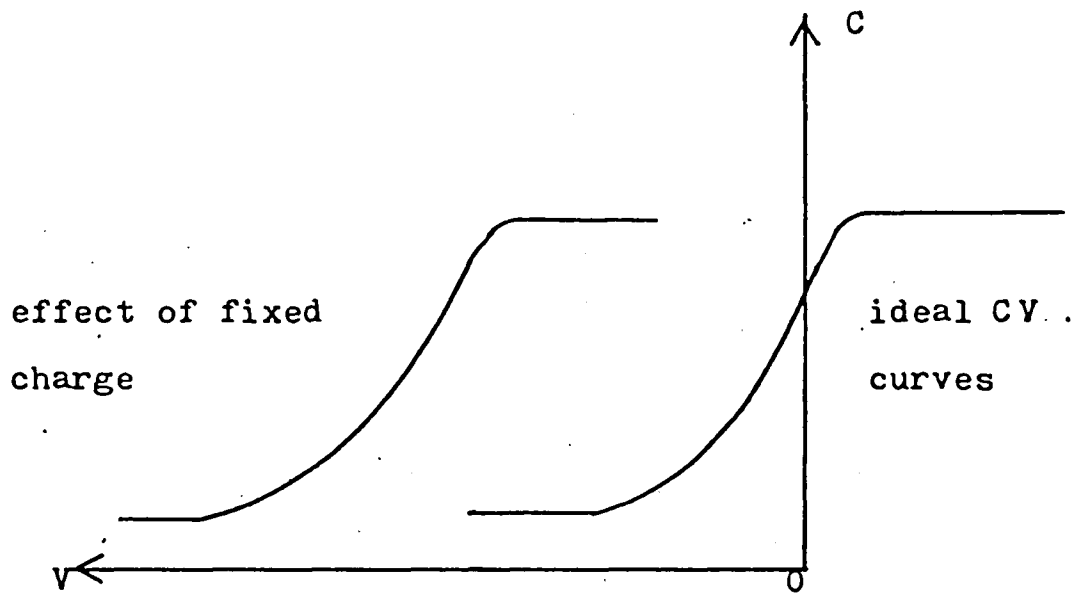


Fig.3 Effect of fixed positive charge on ideal CV curve...

function difference in order to bring about a flat band condition (i.e. no charge induced in the semiconductor) we have to apply a negative voltage to the metal, as shown in Fig. 4B. With increasing negative voltage, more negative charge is applied to the metal which shifts the electric field distribution downwards until the electric field reaching the silicon surface becomes zero. Under this condition the area contained under the electric field distribution is the flat band voltage (V_{FB}).

From Poisson's equation

$$V_{FB} = \frac{-x_1 Q}{K_0 \epsilon_0} = - \frac{x_1}{x_0} \frac{Q}{C_0} \quad (1)$$

Q = Density of sheet charge

V_{FB} = Flat band voltage

x_1 = Location of sheet charge

x_0 = Oxide thickness

C_0 = Oxide capacitance

$K_0 \epsilon_0$ = Permittivity of SiO_2

The more general case of an arbitrary space charge distribution within the SiO_2 is illustrated in Fig. 4C and the flat band voltage is

$$V_{FB} = - \frac{1}{C_0} \int_{x_0}^{x_1} \frac{x}{x_0} \rho(x) dx \quad (2)$$

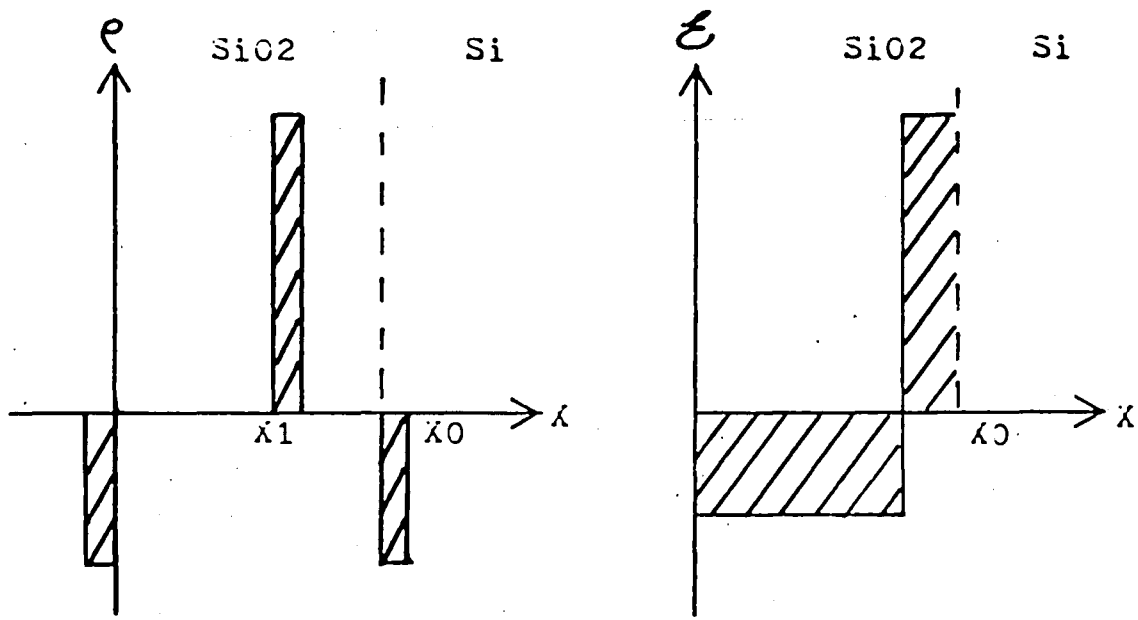


Fig. 4A Effect of charge within the insulator .

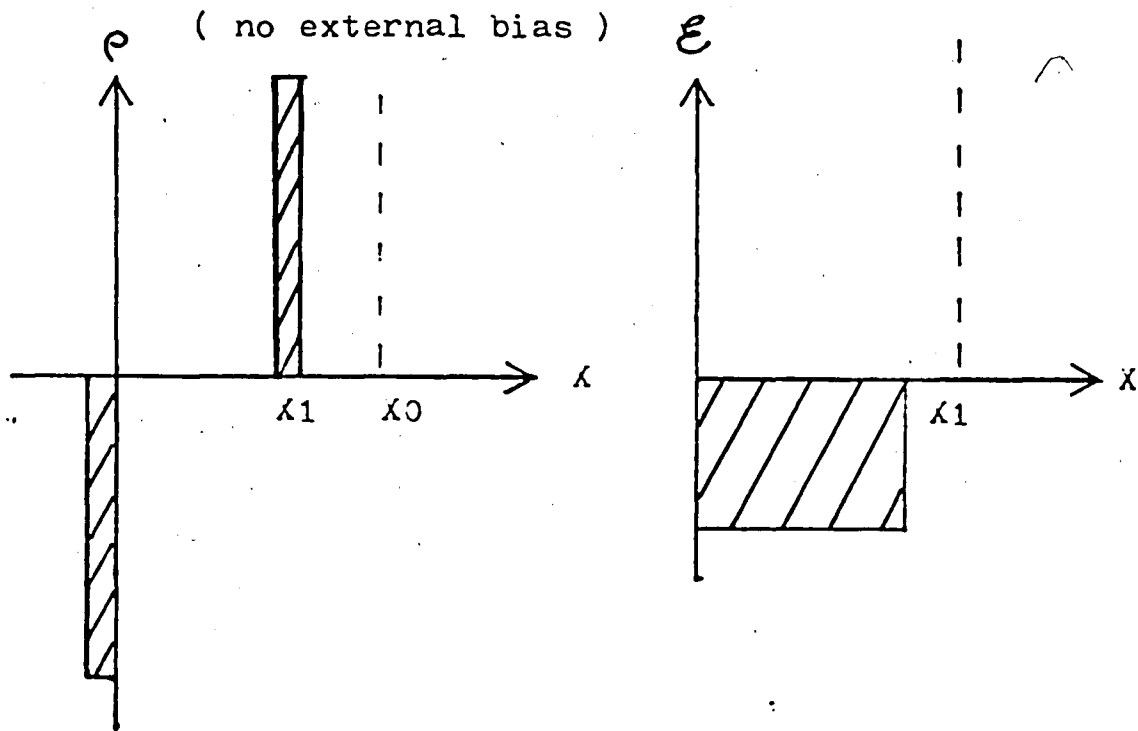


Fig. 4B Effect of charge within the insulator .

(flat band condition)

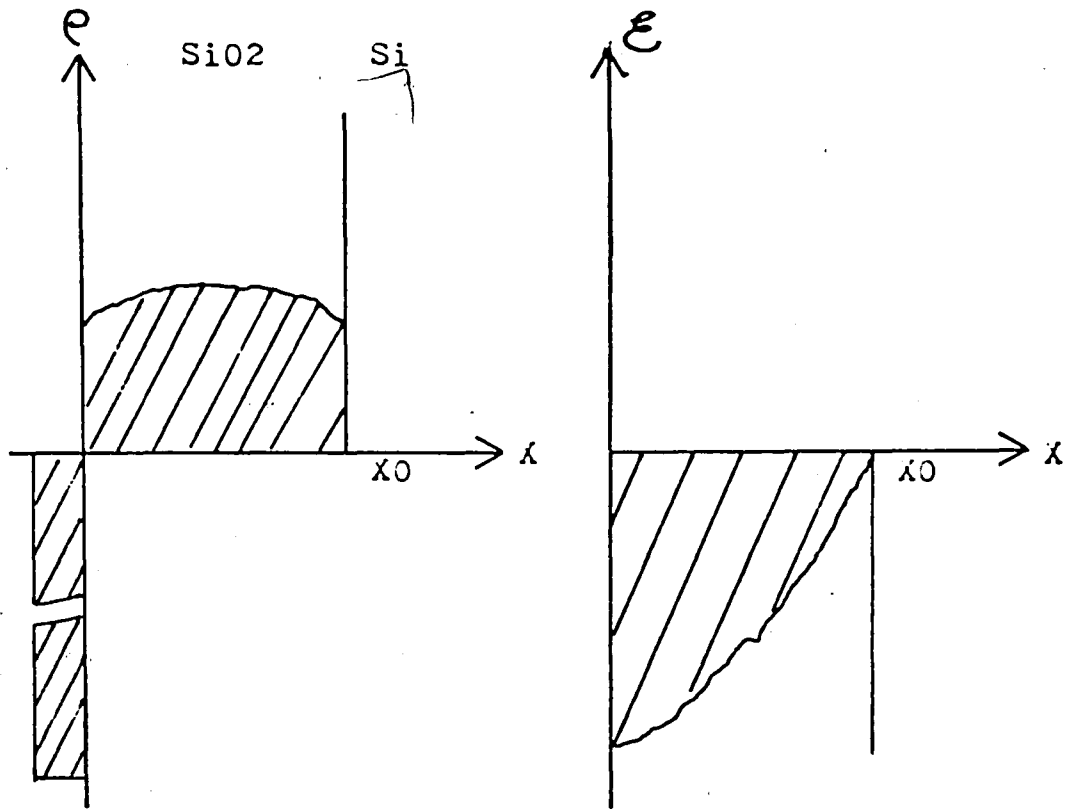


Fig. 4C Effect of an arbitrary space charge distribution within the insulator .

$\rho(x)$ = charge density

Thus the flat band voltage not only depends on the density of the sheet charge but also on its location within the SiO_2 . If the fixed charge is next to the metal, it will induce no image charge in the Si and therefore will have no effect on the semiconductor surface. In the other extreme, when the sheet charge is located next to the semiconductor, it will exert its maximum influence and lead to a flat band voltage of

$$V_{\text{FB}} = - \frac{Q}{C_0}$$

The location of this fixed charge has been measured by many workers, Deal,^[2] Laverty,^[9] Ryan,^[9] Hess,^[6] and Pike.^[8] All agree that most of the charge is located within 200 Angstroms of the Si-SiO₂ interface.

This fixed charge has some distinct properties which are summarized as follows:

- 1) The charge is fixed. It cannot be charged or discharged with externally applied biases.
- 2) It is unchanged under the conditions that would lead to the motion of sodium ions in the oxide (e.g. temperatures of 150°C, positive bias with an oxide field greater than 10⁵V/cm).
- 3) It is within 200 Angstroms of the SiO₂-Si interface.
- 4) Its density is not significantly affected by the oxide

thickness.

5) The charge density is a strong function of the orientation of the Si crystal.

3. Experimental Details

3.1 Fabrication of MOS Capacitors

The MOS capacitors were fabricated on N type, phosphorous doped, chem-mechanically polished silicon wafers. The wafers were typically 250-400 μm thick, the resistivity was in the range of about 8-15 $\Omega\text{-cm}$, with $\langle 100 \rangle$ surface orientation. The cleaning procedure prior to oxidation is described in detail in Appendix A.

3.2 Oxidation

After the normal cleaning procedure, the samples were oxidized to the desired thickness (nominally 1300 Angstroms) at a temperature of 1130°C in dry oxygen with a flow rate of 500 cc/min for 60 minutes. All the oxidation treatments were carried out in a resistance heated Centigrade three zone furnace containing a fused quartz tube and a Mullite liner.

3.3 Reduction

The oxidized samples were then reduced in a reduction furnace. The flow rates of CO and CO₂ were adjusted to achieve the desired partial pressure (see Appendix B). The reduction system consisted of a resistance heated Lindberg Hevi-Duty three zone furnace and a CO and CO₂ gas mixer system. Since the partial pressure of oxygen in the CO-CO₂ atmosphere depends upon the mole ratio of CO and CO₂ in the gas stream, a mixer system was devised which allowed flow rate measurement of each gas individually, which were then thoroughly mixed before they entered the furnace. The gas mixer employed in this experiment was similar to the one used by Fowkes and Hess,^[3,6] except for the addition of three extra drying tubes to the system (Fig. 5). The oxidized samples were reduced in the reduction furnace at a temperature of 910°C for 5 hours. The 5 hours reduction time was shown by Hess^[6] to be the optimum time to reach a saturated value for the oxide charge.

3.4 Reoxidation

After reduction, the samples were reoxidized in the oxidation furnace at a temperature of 925°C in dry oxygen at a flow rate of 1000 cc/min; one sample was processed for each of the different reoxidation times.

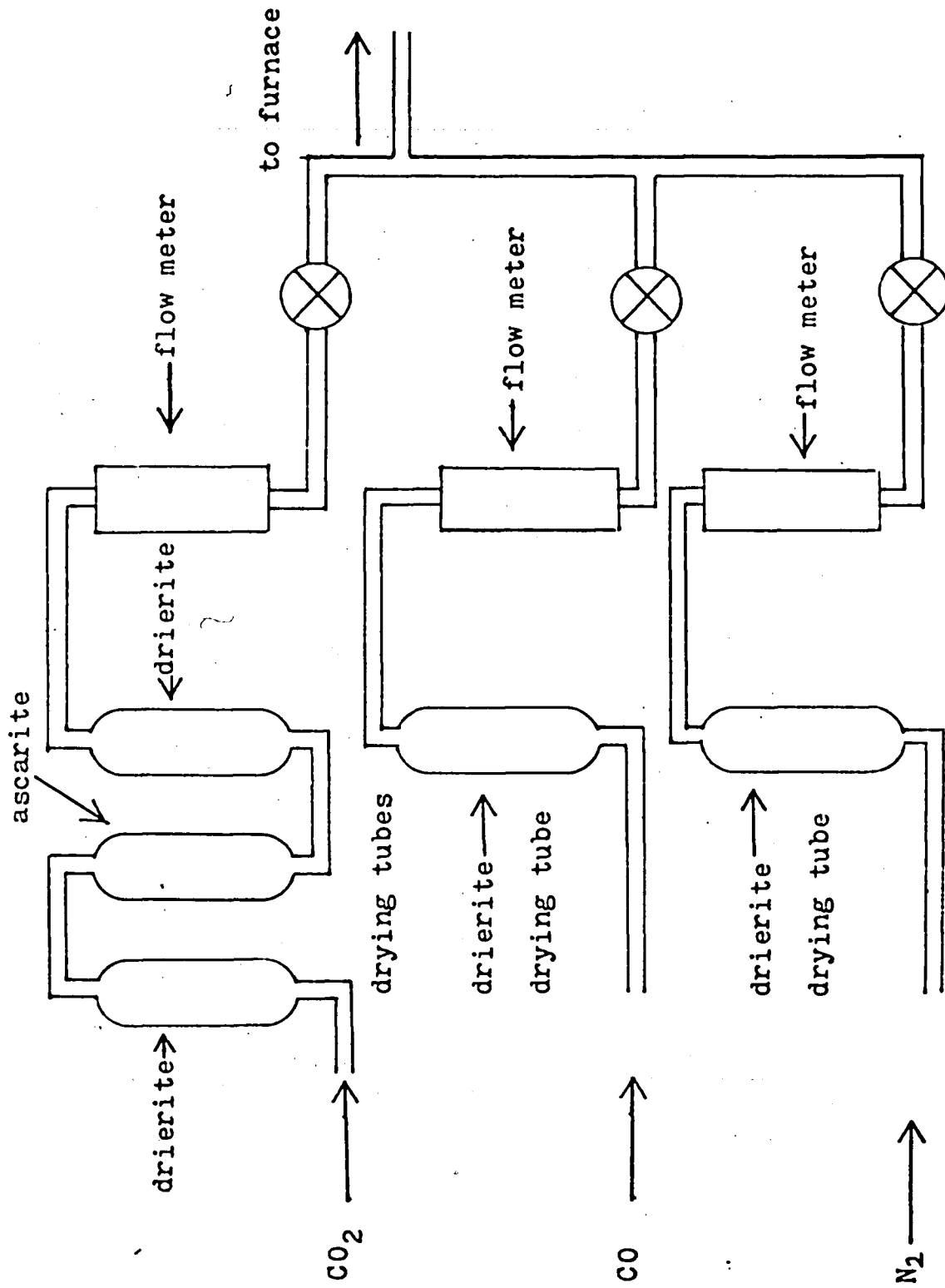


Fig. 5 Gas mixture for the reduction system .

3.5 Deposition of Metal

Aluminum (99.9%) was evaporated from heated tungsten filaments onto the front of the samples in a sputter-ion pumped vacuum system at approximately 10^{-6} torr. A photolithographic process was used to define a circular area on the metal of the MOS capacitor, having a diameter of 5.08×10^{-2} cm².

3.6 Deposition of Back Metal Contact

The back oxide was stripped off the wafer in HF, while the front of the wafer was protected by Apezion black wax. The black wax was subsequently removed with hot trichloroethylene. The samples were then placed into a Veeco high vacuum system utilizing a mechanical roughing pump and an oil diffusion pump. Aluminum contacts were then evaporated on the back of the samples.

3.7 Measurement of Fixed Charge

The fixed charge in the samples was measured at 1MHz by the high frequency capacitance-voltage (c-v) technique. The fixed oxide charge may be determined by the shift in flat band voltage. The set up of the equipment is shown in Fig. 6. It consists of a 1MHz Boonton 71AR-LC meter, a DC ramp generator to provide the bias, an XY recorder and a probe which was gold plated to provide good contact to the aluminum. The samples were placed on the

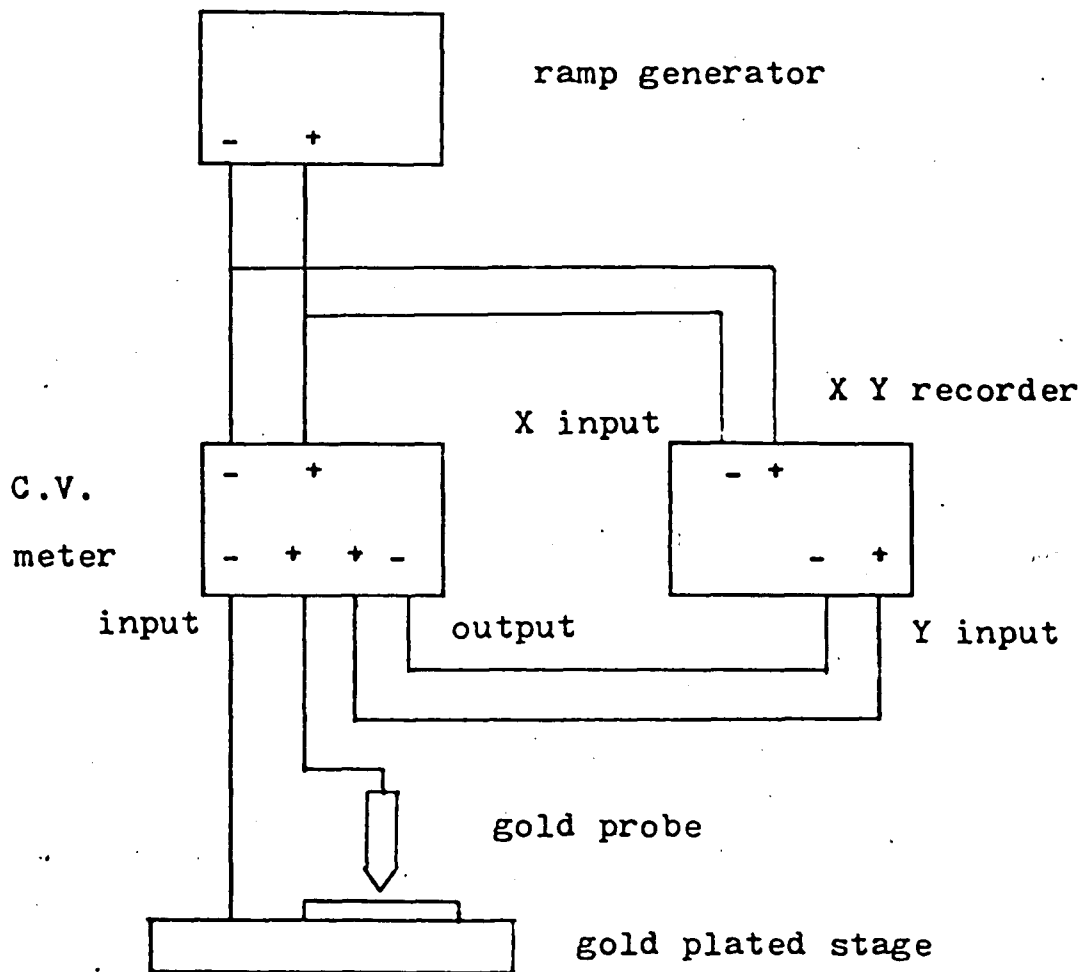


Fig. 6 Experimental setup for C.V. measurement.

stage and after being contacted by the gold probe, the curves were recorded on the XY recorder, in the dark. Typically 5 to 10 measurements were taken from each sample.

4. Results

The oxide charge was measured as a function of the reoxidation time at 910°C . Three different partial pressures (3×10^{-15} atm., 1×10^{-12} atm., 1×10^{-8} atm.) were investigated in these experiments. Fig. 7 shows the oxide charge density as a function of the reoxidation time. It is clear from these results that the non-growth time is a function of the partial pressure of the original reduction process, which explains why Pike's non-growth time was not in agreement with Hess's.

The results of this investigation can be summarized into three areas: the peak oxide charge, non-growth time, and the final charge.

4.1 Peak Oxide Charge

It has been observed that the oxide charge will peak during the beginning of the reoxidation process and will then gradually decrease with time. Pike^[8] reported the same phenomenon, but he could not explain the cause of the peak. The result of the present experiments clearly show that the peak charge is directly

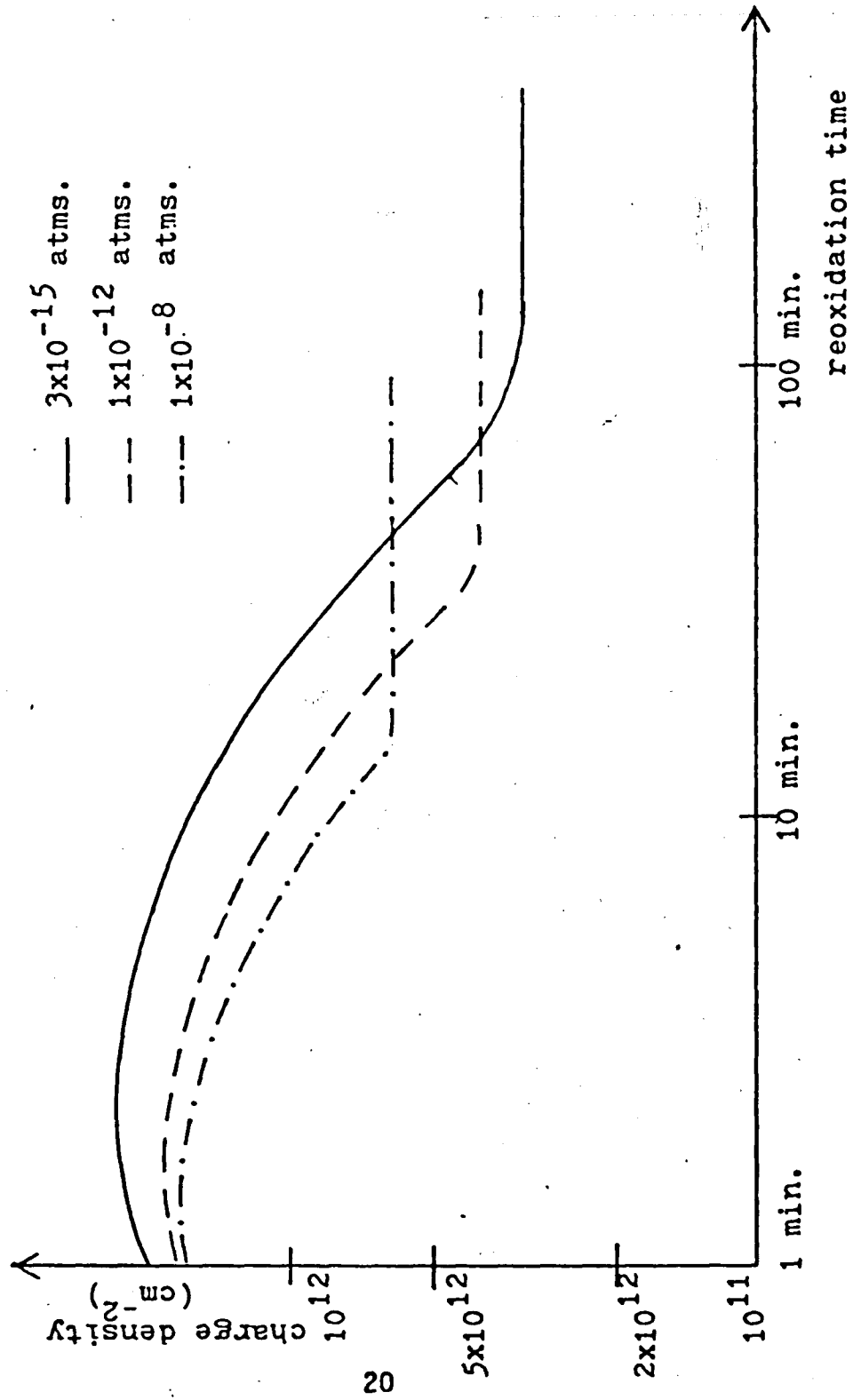


Fig. 7 Charge density as a function of reoxidation time .

related to the partial pressure during the reduction process: the lower the partial pressure the higher the peak oxide charge. In addition, the peak time (time required to reach the peak oxide charge) is also found to be related to the partial pressure. Fig. 8 is a plot of peak time as a function of the oxygen partial pressure.

4.2 Non-Growth Time

Non-growth time is defined as the time required to fill up all the charged oxygen vacancies, which were created by the reduction process. Previous workers have reported a non-growth time of 60 minutes^[3] to 200 minutes.^[8] The non-growth time is directly related to the oxygen partial pressure of the reduction process as shown in Fig. 9. As we have expected, the lower the partial pressure the higher the non-growth time, because more oxygen vacancies are created at lower partial pressures and it is expected that more oxygen or more time will be required to fill up those vacancies. From Pike's work, we know that the non-growth time is not dependent on the thickness of the oxide layer, because, as was pointed out earlier, all the oxide charge is located within 200 Angstroms from the Si-SiO₂ interface. The reoxidation process is strongly temperature dependent, which indicates that the non-growth time is also a function of the temperature.

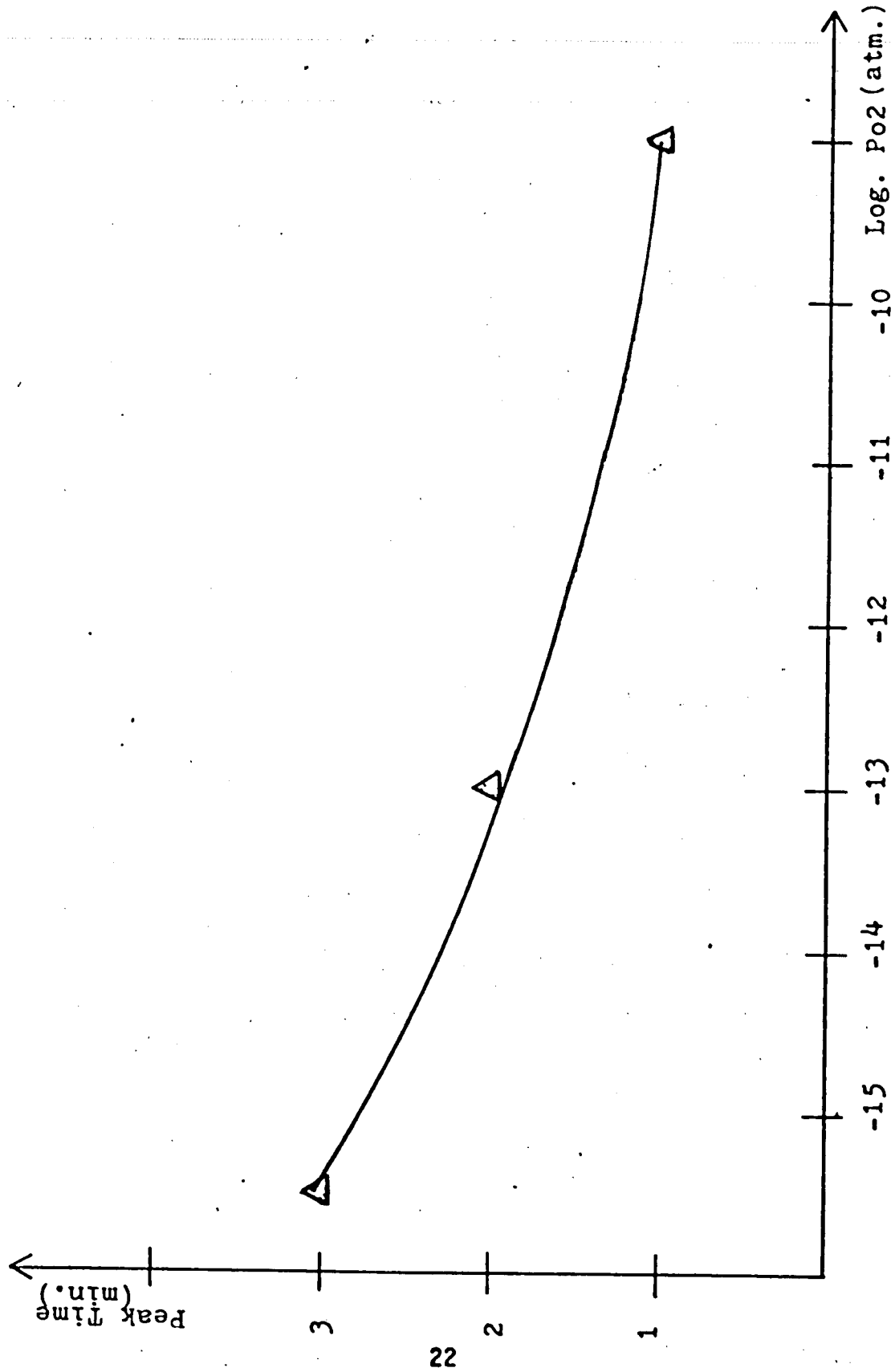


Fig. 8 Peak time as a function of oxygen partial pressure .

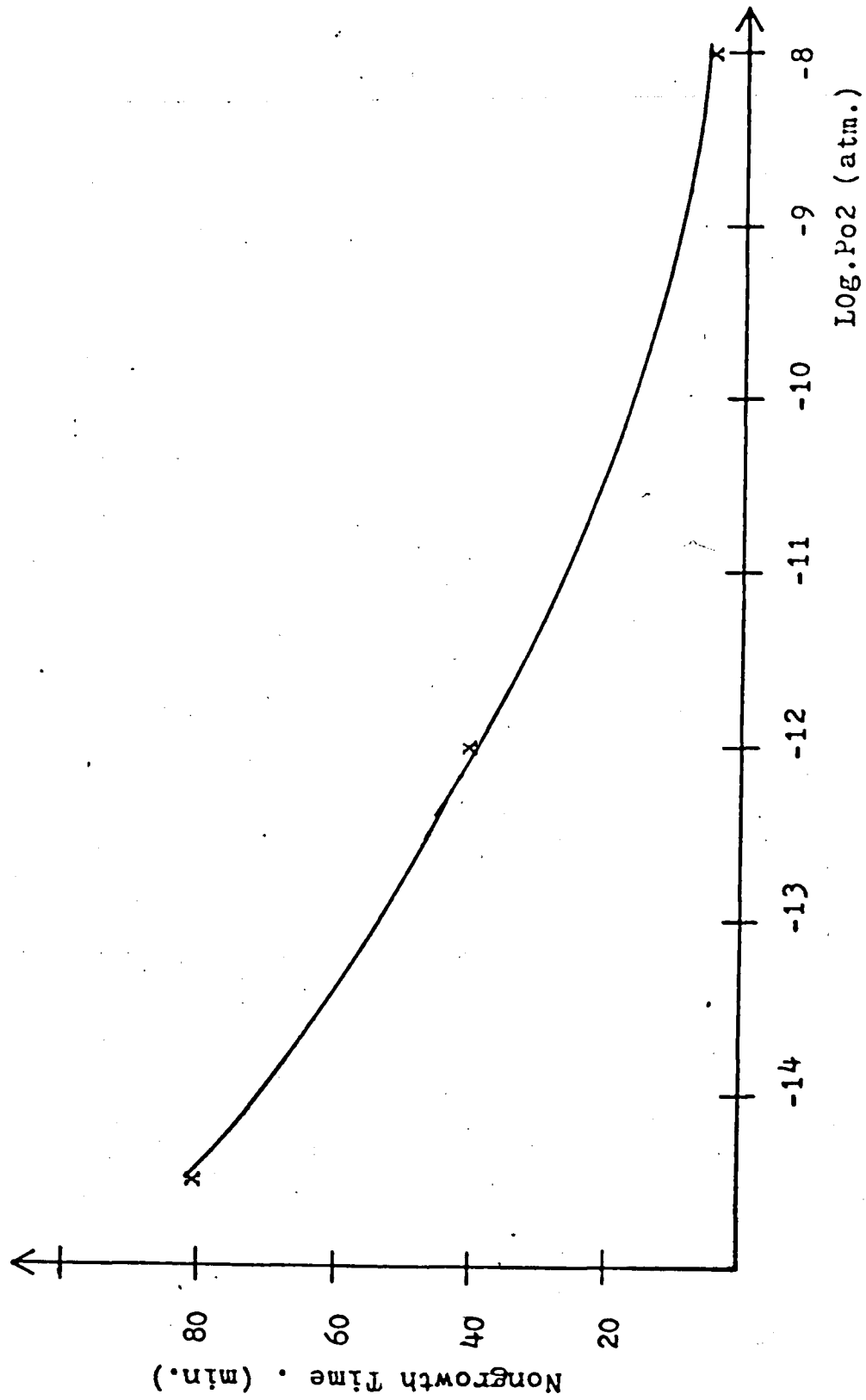


Fig. 9 Nongrowth time as a function of oxygen partial pressure .

Pike^[8] has already demonstrated this point; he reported a non-growth time of 200 minutes at 925° C and 1000 minutes at 850° C.

4.3 Final Oxide Charge

Pike^[8] has reported that the oxide charge density will reduce to its normal low values after the period of the non-growth time. As shown in Fig. 7, this result is not obtained for oxides reduced at higher oxygen partial pressures. Fig. 10 is a plot of final charge as a function of oxygen partial pressure. The difference in final oxide charge is surprising. Many workers^[1,6,3] have agreed that regardless of the previous history of a sample the final heat treatment will determine the value of the fixed charge density, provided only that sufficient time is allowed for the sample to reach steady state. The results of the present experiments, as seen in Fig. 10, do however indicate that the samples have a memory of their previous history: the lower the partial pressure, the lower the final charge.

Fig. 11 shows a plot of oxide thickness as a function of time. After the non-growth period, these samples are observed to grow at a normal rate, as previously reported by Pike.

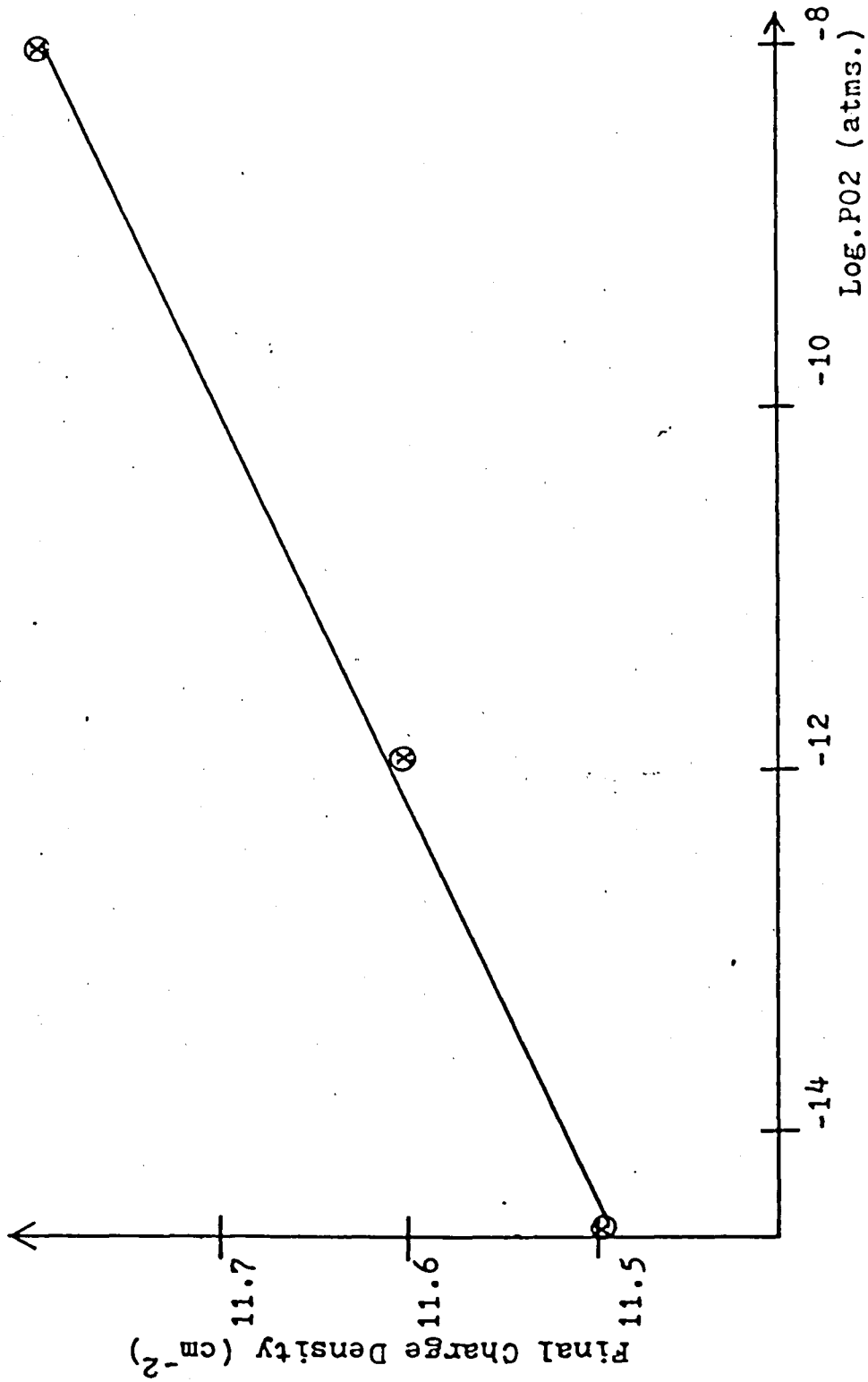


Fig. 10 Final charge density as a function of oxygen partial pressure .

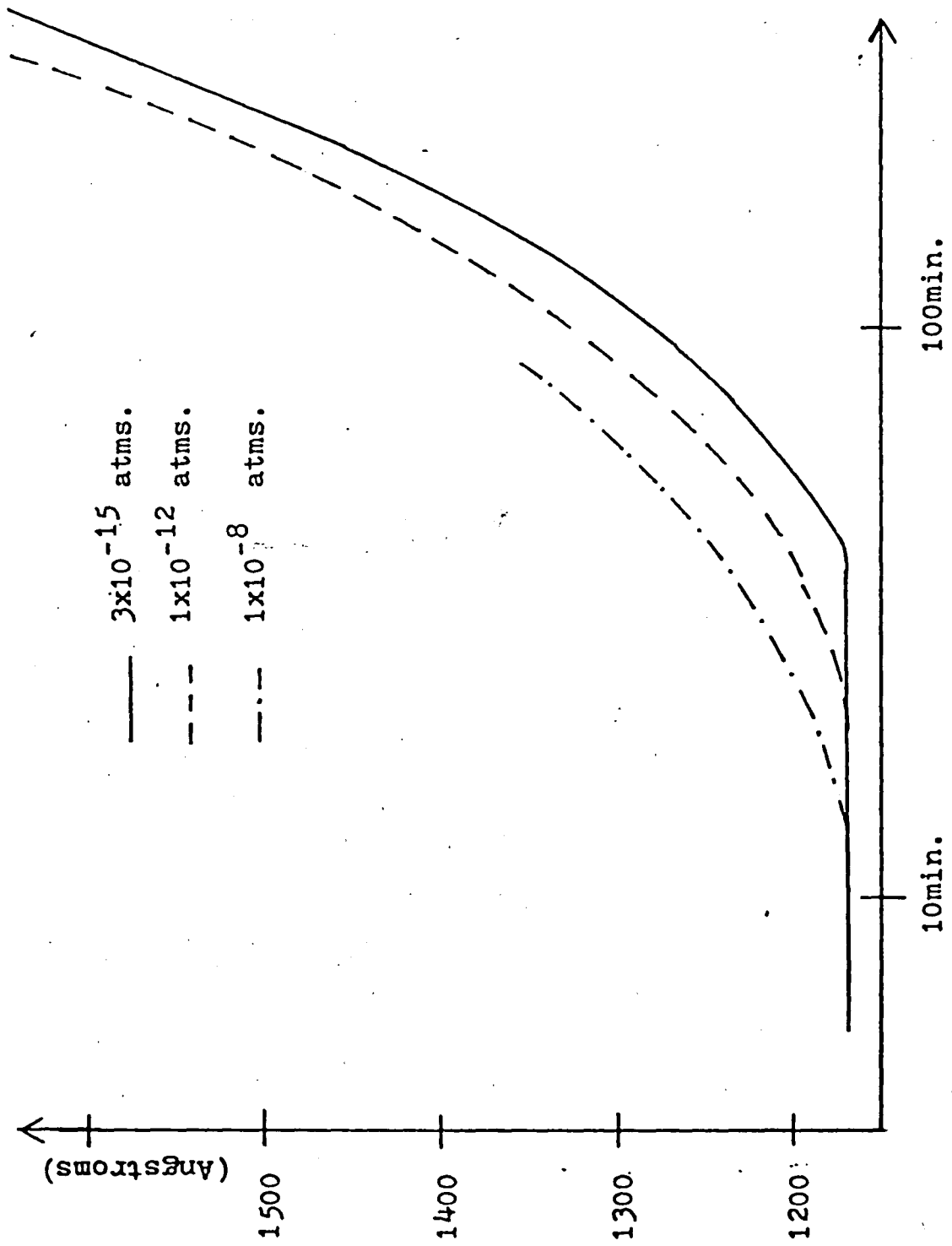


Fig. 11 Oxide thickness as a function of time .

4.4 Fast Surface States

Fig. 12 shows the high frequency (1MHz) c-v curves for different samples. Most samples that have gone through a long re-oxidation time are found to be distorted near the inversion region.

The c-v curves are displaced from their theoretical characteristics by an amount which itself varies with the surface potential, which clearly indicates the existence of fast surface states. If there are states within the forbidden energy gap of the silicon concentrated at the Si-SiO₂ interface, the probability of the occupation of these states will change as a result of the variation in band bending. These states are referred to as fast surface states. The presence of the fast surface states has not much effect on our results, because the observed fast surface states occur near the valence band edge and thus have no influence on flat band voltage.

Fig. 13 is a collection of data which have been reported by different workers (Pike and Hess). It can be seen from Fig. 13, that our results are in good agreement with those of Pike and Hess.

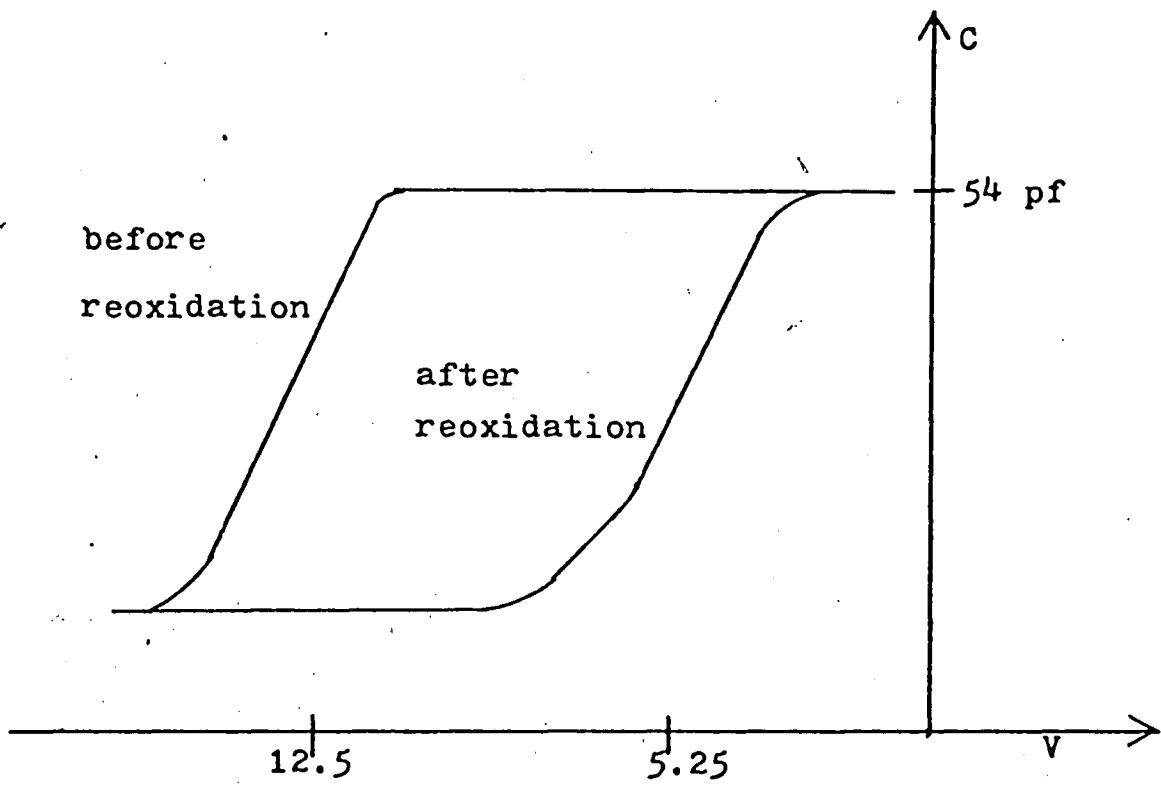


Fig. 12 Distortion of C.V. curves .

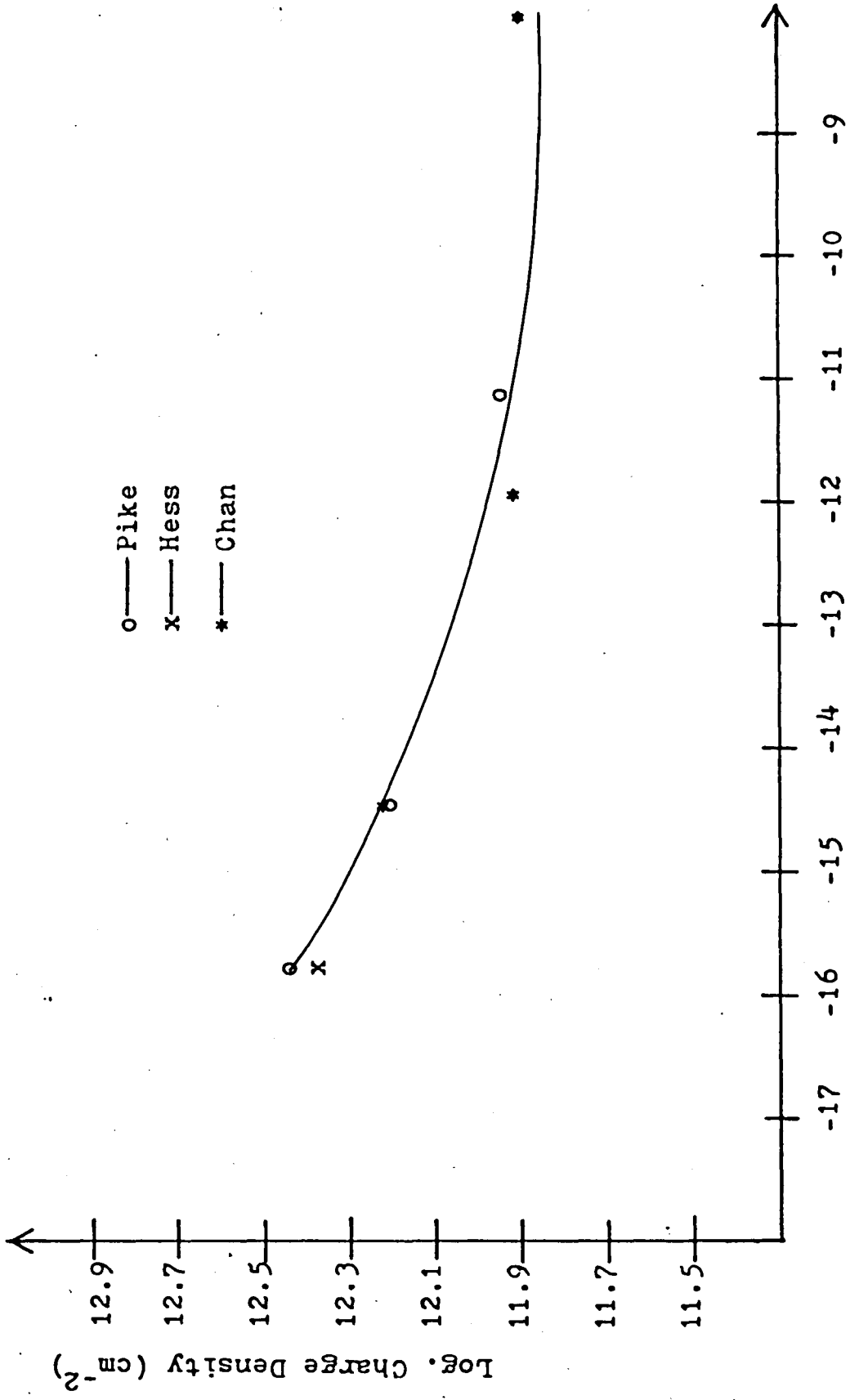


Fig. 13 Charge density as a function of oxygen partial pressure .

5. Discussion

In this investigation we have concentrated our interest on the reoxidation process of reduced oxides. As we have pointed out in the previous chapter, the results of the peak charge and final charge are really unexpected. The data of the non-growth time also gives us additional information of the reoxidation process.

We are going to conclude this investigation by presenting three models to explain the three different phases of the reoxidation process.

5.1 Model for Peak Oxide Charge

Fig. 14A shows a plot of oxide charge density vs. reoxidation time. We have defined the Peak time (t_p) as the time required to reach the peak oxide charge, and ΔQ_p is the difference between peak oxide charge and the oxide charge before reoxidation. ΔQ_p and t_p for four different partial pressures are given in Table I.

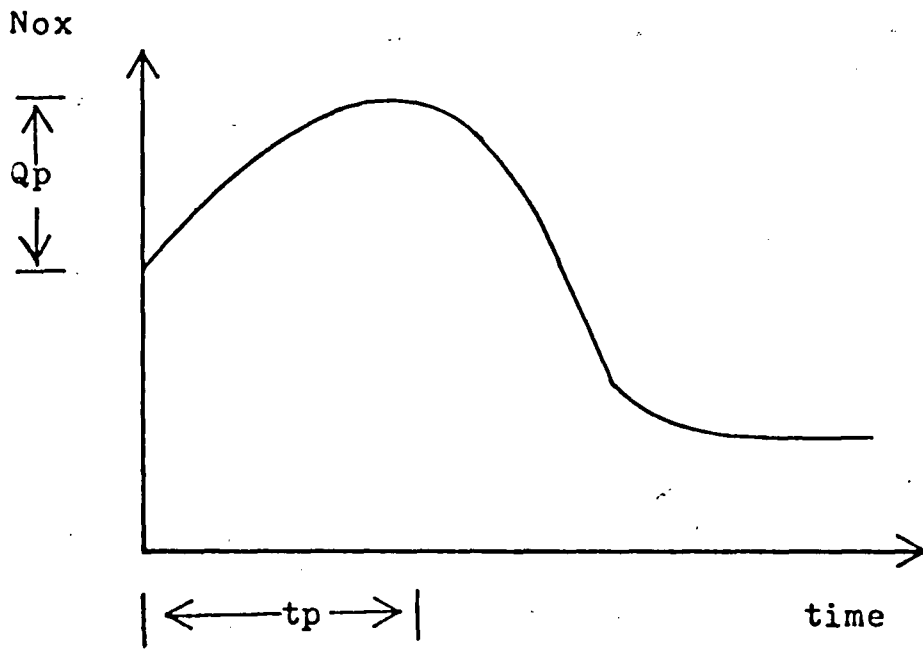


Fig. 14A Charge density as a function of time .

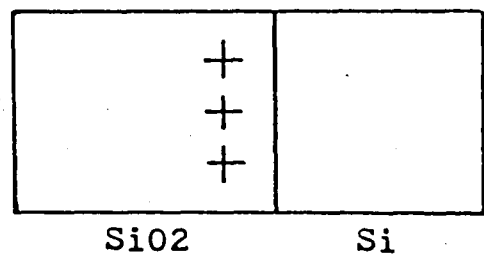


Fig. 14B SiO₂-Si charge distribution before reoxidation .

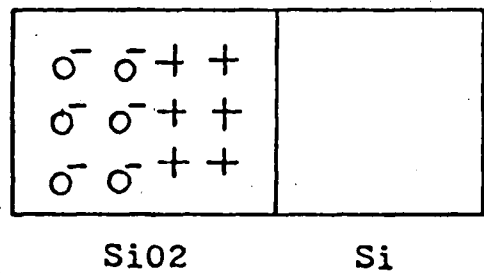


Fig. 14C SiO₂-Si charge distribution after reoxidation .

P_{O_2} (atm.)	t_p (min.)	ΔQ_p (cm^{-2})
8×10^{-13}	4	8×10^{11}
3×10^{-15}	3	8×10^{11}
1×10^{-12}	2	1×10^{12}
1×10^{-8}	1	8.3×10^{11}

TABLE I - Peak Time and ΔQ_p .

ΔQ_p remains almost constant ($8 \times 10^{11} \text{ cm}^{-2}$), except that there is a small difference at the partial pressure 1×10^{-12} atm. ($\Delta Q_p = 1 \times 10^{12} \text{ cm}^{-2}$), which could be an experimental error. The constant ΔQ_p leads us to the conclusion that ΔQ_p is not dependent on the charged oxygen vacancies present in the SiO_2 . To support this hypothesis, we have calculated the amount of oxygen which diffused into the SiO_2 during the time " t_p " (Table II), using published values for the diffusion constant and the solid solubility of oxygen in SiO_2 (see Appendix C for sample calculation).

P_{O_2} (atm.)	t_p (min.)	Amount of O_2 (cm^{-2})
8×10^{-17}	4	5.5×10^{13}
3×10^{-15}	3	4.79×10^{13}
1×10^{-12}	2	3.9×10^{13}
1×10^{-8}	1	2.75×10^{13}

TABLE II-Oxygen Diffusion in SiO_2 .

The data from Table II does indeed support our hypothesis, as is indicated from the calculations, that the amount of oxygen present in the SiO_2 is about 100 times larger than ΔQ_p . Based on this assumption and the experimental data, a model is proposed to describe the reoxidation process up to the time " t_p ". This model is summarized in Figs. 14B, 14C and 14D. We have already pointed out in the previous chapter that all the fixed charge is located within the first 200 Angstroms from the Si- SiO_2 interface (Fig. 14B), so it is reasonable to assume that the fixed charge has no appreciable effect on the remaining thickness of the SiO_2 .

During the reoxidation, oxygen atoms diffuse into the SiO_2 , just as in an ordinary oxidation process. The incoming oxygen atoms become ionized and form a localized negative charge distributed evenly in the entire 1100 Angstroms SiO_2 (Fig. 14C).

After losing one of the electrons to the incoming oxygen atoms, the charged oxygen vacancies become doubly ionized. The sudden increase in charge near the interface during the peak time is a result of the doubly ionized charged oxygen vacancies.

The above model has failed to explain the difference in peak time (t_p). If we assume a constant diffusion coefficient and based on our previous argument, all the peak charge should appear at the same time. The difference in peak time leads us to believe that the actual diffusion coefficient is altered by the reduction process. Of course, this is only a theory; further experimental work has to be done to prove this hypothesis. One proposal is to measure the diffusion coefficient of different reduced samples.

5.2 Model for Non-Growth Time

Reduced oxides have shown a large non-growth time, whose cause is obscure.

Fig. 15A is a plot of charge density vs. reoxidation time. ΔQ_2 is the difference between peak oxide charge and final charge. ΔQ_2 and TN (non-growth time) are tabulated in Table III.

P_{O_2} (atm.)	TN (min.)	ΔO_2 (cm^{-2})
8×10^{-17}	200	2.85×10^{12}
3×10^{-15}	100	2×10^{12}
1×10^{-12}	40	1.44×10^{12}
1×10^{-8}	15	9.9×10^{11}

TABLE III - Non-growth Time and ΔO_2 .

As shown from Table II, III and Fig. 15A, the non-growth time (TN) is much larger than the peak time (t_p). We will simplify the problem by neglecting the peak time (Fig. 15B).

We have demonstrated in the previous section (5.1) that all the oxygen vacancies in the first 1100 Angstroms are filled during the peak time (t_p). Therefore the first 1100 Angstroms has no sufficient contribution to the rest of the reoxidation process. Hess has demonstrated in his work that there are a large number of charged oxygen vacancies in the 200 Angstroms SiO_2 film, the number of charged oxygen vacancies being proportional to the oxygen partial pressure during reduction. During the reoxidation process, the charged oxygen vacancies are filled by oxygen atoms via diffusion. Diffusion is a continuous process, that means all the oxygen vacancies in the SiO_2 have to be filled before the oxygen atoms can reach the silicon to form new SiO_2 .

The long non-growth time leads us to believe that most of the charged oxygen vacancies are in substitutional sites. Hess and Pike have demonstrated that it only takes a fraction of the non-growth time to fill up the entire 1000 Angstroms SiO_2 film with oxygen via interstitial diffusion. Substitutional diffusion is a very slow process compared with interstitial diffusion, the existence of an electric field in the interface also contributed to the long non-growth time by pushing ionized oxygen atoms away from the interface. Therefore the effective diffusion coefficient is still much smaller than the interstitial diffusion coefficient (we have lumped the electric field effect and the substitutional diffusion coefficient into one constant). The effective coefficient is calculated from the experiment data and is listed in Table IV.

P_{O_2} (atm.)	TN (min.)	Effective Diffusion Coefficient ($\text{cm}^2/\text{sec.}$)
8×10^{-17}	200	5.3×10^{-12}
3×10^{-15}	100	5.2×10^{-12}
1×10^{-12}	40	5.13×10^{-12}
1×10^{-8}	50	8.8×10^{-12}

TABLE IV - Effective Diffusion Coefficient.

The results from Table IV do support our theory that the effective diffusion coefficient is about $5.2 \times 10^{-12} \text{ cm}^{-2}/\text{sec}$, which is in close agreement with some of the published data for substitutional diffusion coefficients of oxygen in SiO_2 . In order to achieve a oxygen partial pressure of 1×10^{-8} atm., we need a ratio of CO/CO_2 about 1000 to 1, which is limited by the accuracy of our equipment. Therefore the accuracy of these data is somewhat poor.

The above is a rather qualitative model and more work has to be done to verify the effective diffusion coefficient. Nevertheless, this model does give us a good understanding and a reasonable explanation for the non-growth time.

5.3 Final Charge

After the non-growth time (TN), the oxides assume their normal growing condition. The final charge density is found to be a function of the initial oxygen partial pressure during reduction (Fig. 10).

At this moment, we are unable to explain the cause of the difference in final charge. We believe the final charge is caused by the excess ionized oxygen atoms in the SiO_2 , but we are unable to explain the existence of such ionized oxygen atoms after the samples have gone through such a long reoxidation time.

Appendix A

Cleaning of Si Wafers

The samples were degreased by boiling in trichloroethylene, acetone and methanol for about 5 minutes each. After rinsing in deionized water, the samples were further degreased by boiling in H_2SO_4 containing approximately 20% of H_2O_2 . Next the samples were rinsed in deionized water, etched until hydrophobic in HF and again rinsed in deionized water. The samples were then preoxidized at $1130^\circ C$ in wet oxygen for about 60 minutes. This oxide was then etched until hydrophobic in HF to remove surface contamination and the samples were rinsed in deionized water.

Appendix B

TEMP	Po ₂ (atm.)	CO ₂ (cc/min)	CO (cc/min)
910°C	1 x 10 ⁻¹⁸	54	746
	4 x 10 ⁻¹⁷	251	549
	3 x 10 ⁻¹⁵	639	161
	2.5 x 10 ⁻¹⁴	736	64
	1.6 x 10 ⁻¹³	773	27
	1 x 10 ⁻¹²	789	11
	1 x 10 ⁻⁸	799.89	0.11

TABLE V

Oxygen partial pressure as a function of the flow rates.

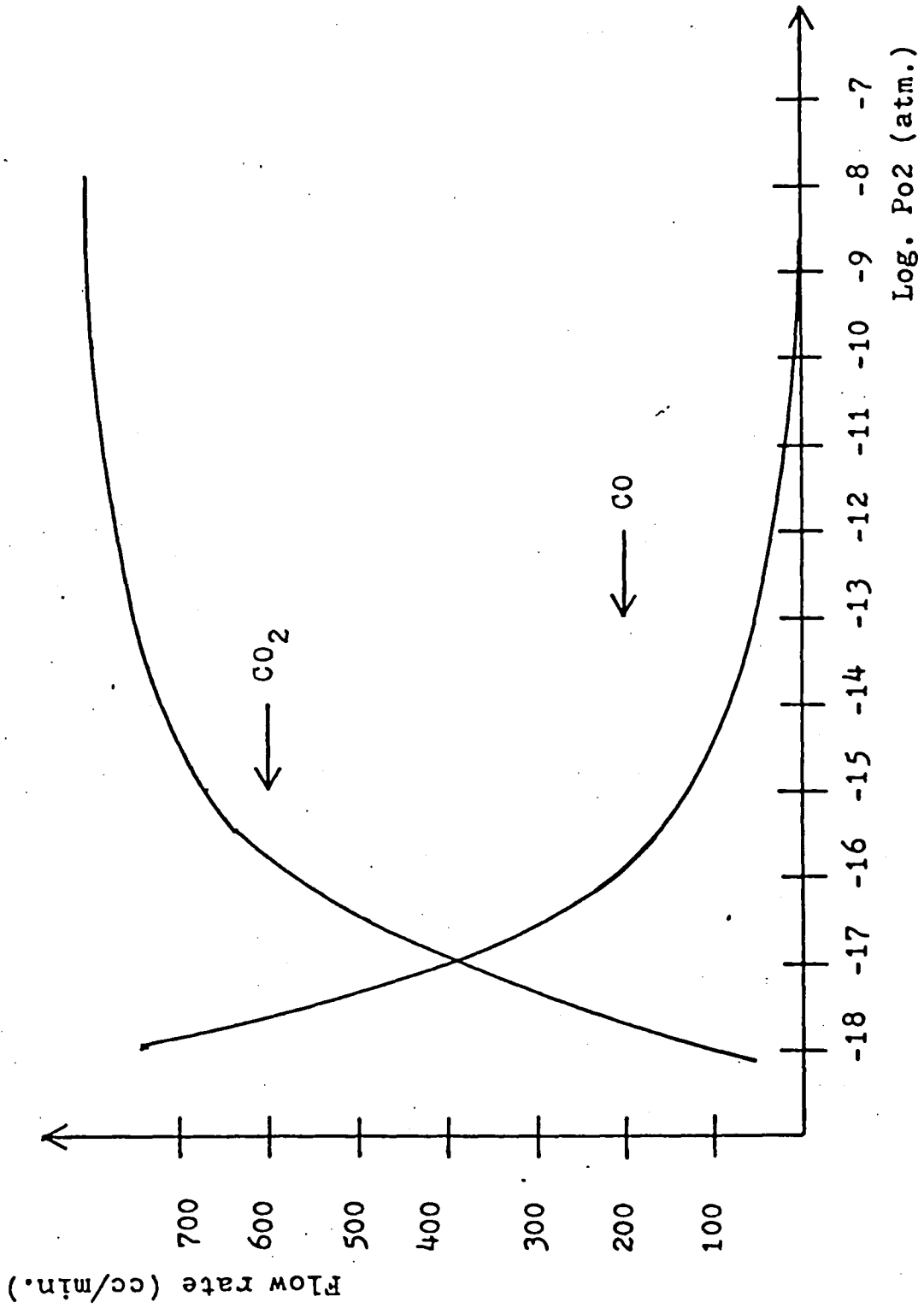


Fig. 15 Oxygen partial pressure as a function of the flow rate .

Appendix C

Amount of oxygen atoms diffused into SiO₂ .

$$Q = 2N_0(Dxt/3.14)^{1/2}$$

N₀ = surface concentration

$$= 1 \times 10^{16} / \text{cm}^2$$

D = diffusion coefficient

$$= 1 \times 10^{-7} \text{ cm}^2 / \text{sec.}$$

t = time

$$= 4 \text{ min.}$$

$$Q = \underline{5.5 \times 10^{13} / \text{cm}^2}$$

REFERENCES

- [1] Grove, A. S., Physics and Technology of Semiconductor Devices, John Wiley and Sons, Inc., New York, 1969, Chapter 12, pp. 334-353.
- [2] Deal, B. E., Sklar, M., and Grove, A. S., J. Electrochem. Soc., vol. 114 (1967) p. 266.
- [3] Fowkes, F. M. and Hess, D. W., Appl. Phys. Lect., vol. 22 (1973) p. 377.
- [4] Lindmayer, J., Solid State Electron., vol. 9 (1966) p. 225.
- [5] Revesz, A. G., and Evans, R. J., J. Phys. Chem. Solids, m M vol. 28 (1967) p. 197.
- [6] Hess, D. W., Unpublished Ph. D. Thesis, Lehigh University (1973).
- [7] Kiddon, John, Unpublished Master Thesis, Lehigh University (1979).
- [8] Pike, Douglas A., Unpublished Master Thesis, Lehigh University (1974).
- [9] Laverty, S. J. and Ryan, W. D., Int. J. Electron., vol. 26 (1969) p. 519.

Vita

Cheong-Fat Chan was born in Hong Kong on January 19, 1952 to Mr. and Mrs. Ying-Ting Chan. He graduated from Cain High School, Hong Kong in 1971. Mr. Chan came to the United States and attended Broome Community College in 1972, receiving an Associate Degree in Electrical Technology in June 1974. He entered State University of New York at Binghamton in 1974, where he graduated with high honors and received a degree in Bachelor of Technology in Electrical Engineering in May 1976. He entered Lehigh University in September 1976. Since then, he has been a teaching assistant in Electrical Engineering at Lehigh University.